J|A|C|S ARTICLES

Published on Web 03/26/2009

Coupled Growth and Division of Model Protocell Membranes

Ting F. Zhu[†,‡] and Jack W. Szostak*[,†]

Howard Hughes Medical Institute, and Department of Molecular Biology, Massachusetts General Hospital, Boston, Massachusetts 02114, and Harvard-MIT Division of Health Sciences and Technology, Massachusetts Institute of Technology, Cambridge, Massachusetts 02139

Received February 5, 2009; E-mail: szostak@molbio.mgh.harvard.edu

Abstract: The generation of synthetic forms of cellular life requires solutions to the problem of how biological processes such as cyclic growth and division could emerge from purely physical and chemical systems. Small unilamellar fatty acid vesicles grow when fed with fatty acid micelles and can be forced to divide by extrusion, but this artificial division process results in significant loss of protocell contents during each division cycle. Here we describe a simple and efficient pathway for model protocell membrane growth and division. The growth of large multilamellar fatty acid vesicles fed with fatty acid micelles, in a solution where solute permeation across the membranes is slow, results in the transformation of initially spherical vesicles into long thread-like vesicles, a process driven by the transient imbalance between surface area and volume growth. Modest shear forces are then sufficient to cause the thread-like vesicles to divide into multiple daughter vesicles without loss of internal contents. In an environment of gentle shear, protocell growth and division are thus coupled processes. We show that model protocells can proceed through multiple cycles of reproduction. Encapsulated RNA molecules, representing a primitive genome, are distributed to the daughter vesicles. Our observations bring us closer to the laboratory synthesis of a complete protocell consisting of a self-replicating genome and a self-replicating membrane compartment. In addition, the robustness and simplicity of this pathway suggests that similar processes might have occurred under the prebiotic conditions of the early Earth.

Introduction

One of the major challenges confronting attempts to synthesize artificial forms of life is understanding how a structurally simple protocell could accomplish the apparently complex biological function of self-replication in the absence of evolved biological machinery.[1] A self-replicating protocell requires, minimally, two essential components: a self-replicating genome such as an RNA polymerase ribozyme[2] or a chemically replicating nucleic acid, and a membrane compartment that can grow and divide.[3,4] We have recently demonstrated the spontaneous copying of a vesicle-encapsulated genetic template,[5] and the thermal strand separation of an encapsulated DNA duplex,[6] suggesting that the spontaneous replication of encapsulated genetic polymers may be possible. Here we describe simple processes that lead to the efficient growth and division of model protocell membranes.

Fatty acid vesicles have long been studied as a model system for protocell membranes,[3,5,7−9] as fatty acids and similar membrane-forming amphiphilic molecules have been isolated from meteorites and synthesized under simulated prebiotic conditions.[10−16] The physical properties of small (typically 100 nm in diameter) unilamellar fatty acid vesicles have been studied in depth.[3,5,6,17−20] For a population of vesicles to grow, fresh lipid molecules must be supplied. Pioneering studies in the laboratory of P. L. Luisi showed that when vesicles in a buffered solution are fed with alkaline fatty acid micelles (which become

[†] Massachusetts General Hospital.
[‡] Massachusetts Institute of Technology.

(1) Szostak, J. W.; Bartel, D. P.; Luisi, P. L. *Nature (London)* **2001**, *409*, 387–390.
(2) Johnston, W. K.; Unrau, P. J.; Lawrence, M. S.; Glasner, M. E.; Bartel, D. P. *Science* **2001**, *292*, 1319–1325.
(3) Hanczyc, M. M.; Fujikawa, S. M.; Szostak, J. W. *Science* **2003**, *302*, 618–622.
(4) Hanczyc, M. M.; Szostak, J. W. *Curr. Opin. Chem. Biol.* **2004**, *8*, 660–664.
(5) Mansy, S. S.; Schrum, J. P.; Krishnamurthy, M.; Tobe, S.; Treco, D. A.; Szostak, J. W. *Nature (London)* **2008**, *454*, 122–125.
(6) Mansy, S. S.; Szostak, J. W. *Proc. Natl. Acad. Sci. U.S.A.* **2008**, *105*, 13351–13355.
(7) Gebicki, J. M.; Hicks, M. *Nature (London)* **1973**, *243*, 232–234.
(8) Hargreaves, W. R.; Deamer, D. W. *Biochemistry* **1978**, *17*, 3759–3768.
(9) Walde, P.; Wick, R.; Fresta, M.; Mangone, A.; Luisi, P. L. *J. Am. Chem. Soc.* **1994**, *116*, 11649–11654.
(10) Deamer, D. W. *Nature (London)* **1985**, *317*, 792–794.
(11) Deamer, D. W.; Pashley, R. M. *Origins Life Evol. Biosphere* **1989**, *19*, 21–38.
(12) McCollom, T. M.; Ritter, G.; Simoneit, B. R. *Origins Life Evol. Biosphere* **1999**, *29*, 153–166.
(13) Naraoka, H.; Shimoyama, A.; Harada, K. *Origins Life Evol. Biosphere* **1999**, *29*, 187–201.
(14) Nooner, D. W.; Gibert, J. M.; Gelpi, E.; Oro, J. *Geochim. Cosmochim. Acta* **1976**, *40*, 915–924.
(15) Rushdi, A. I.; Simoneit, B. R. *Origins Life Evol. Biosphere* **2001**, *31*, 103–118.
(16) Yuen, G. U.; Kvenvold, K. A. *Nature (London)* **1973**, *246*, 301–302.
(17) Chen, I. A.; Roberts, R. W.; Szostak, J. W. *Science* **2004**, *305*, 1474–1476.
(18) Chen, I. A.; Szostak, J. W. *Biophys. J.* **2004**, *87*, 988–998.
(19) Chen, I. A.; Szostak, J. W. *Proc. Natl. Acad. Sci. U.S.A.* **2004**, *101*, 7965–7970.
(20) Sacerdote, M. G.; Szostak, J. W. *Proc. Natl. Acad. Sci. U.S.A.* **2005**, *102*, 6004–6008.

thermodynamically unstable at lower pH), the lipid molecules can either be incorporated into pre-existing membranes (leading to growth),[3,18,21] or self-assemble into new vesicles.[21−25] While vesicle growth by feeding with fatty acid micelles can be very efficient,[3] vesicle division by extrusion through small pores results in the loss of a substantial fraction of the encapsulated vesicle contents to the environment.[3,4] Furthermore, it is unlikely for an analogous vesicle extrusion process to occur in a prebiotic scenario on the early Earth, because vesicle extrusion by flowing suspended vesicles through a porous rock would require both the absence of any large pores or channels, and a very high pressure gradient (text S1, Supporting Information). The possible spontaneous division of small unilamellar vesicles after micelle addition has been discussed,[23,26] and electron microscopy has revealed structures that are possible intermediates of growth and division.[27] However, the inheritance of the contents and membranes of parental vesicles by the newly formed vesicles has not been experimentally confirmed.

In contrast to the small unilamellar vesicles discussed above, fatty acid vesicles that form spontaneously by the rehydration of dry fatty acid films, or by the acidification of concentrated solutions of micelles, tend to be large (several microns in diameter) and multilamellar.[3,8] Until recently, we have avoided using multilamellar vesicles for laboratory studies, because populations of such vesicles are so heterogeneous that quantitative studies of growth and division are difficult. To address this problem, we developed a simple procedure for the preparation of large (∼4 μm in diameter) monodisperse multilamellar vesicles by large-pore dialysis.[28] This gentle procedure preserves the original physical properties (e.g., multilamellar structure, volume, and osmolarity) of the large multilamellar vesicles. When we added fatty acid micelles to large monodisperse multilamellar vesicles prepared in this manner, we were able to directly observe a novel and unexpected mode of vesicle growth that allows for efficient division under modest shear forces.

Materials and Methods

Preparation of Large Monodisperse Multilamellar Vesicles. Fatty acids and fatty acid derivatives were obtained from Nu-chek Prep (Elysian, MN). Fluorescent dyes were obtained from Molecular Probes, Inc. (Eugene, OR). Oleate vesicles were prepared by resuspending a dried film of oleic acid in 0.2 M Na-bicine (Sigma-Aldrich, St. Louis, MO) containing 2−10 mM HPTS at pH 8.5, to a final concentration of 10 mM oleic acid. The vesicle suspension was vortexed briefly and tumbled overnight. Dilutions of vesicles were made using buffers containing fatty acids above the critical aggregate concentration (cac; ∼80 μM for oleic acid, ∼4 mM for myristoleic acid, and ∼30 mM for decanoic acid), to avoid vesicle dissolution. The method for the preparation of large (∼4 μm in diameter) monodisperse multilamellar vesicles by extrusion and large-pore dialysis has been described.[28] Briefly, extrusion of polydisperse vesicles through 5-μm diameter pores eliminates vesicles larger than 5 μm in diameter. Dialysis of extruded vesicles against 3-μm pore-size polycarbonate membranes eliminates vesicles smaller than 3 μm in diameter, leaving behind a population of monodisperse vesicles with a mean diameter of ∼4 μm. The wash buffer for the dialysis of fatty acid vesicles was prepared by resuspending 10 mM oleic acid in 0.2 M Na-bicine buffer at pH 8.5 but without fluorescent dye, to maintain the lipid concentration above the cac and avoid vesicle dissolution during dialysis. Thus the resultant vesicle population contained large monodisperse vesicles encapsulating fluorescent dye and smaller ones that were dye-free (since they are not fluorescent, their presence does not affect the imaging and the counting of large dye-labeled vesicles by fluorescence microscopy). Oleate vesicles in 0.2 M ammonium acetate or 0.2 M Na-glycine were prepared and dialyzed using the same method. Decanoate vesicles were prepared and dialyzed in a water bath above the melting temperature of decanoic acid, at 50 °C. Vesicles encapsulating fluorescently tagged RNA, 5′-DY547-AAA AAA AAA A-3′ (Dharmacon, Chicago, IL), were prepared by dissolving 0.5 mM of the fluorescently tagged RNA in 0.2 M Na-bicine buffer at pH 8.5, followed by the vesicle preparation and dialysis procedures described above. Dialysis was conducted under argon to avoid oxidation of dye-labeled RNA, and RNase-free reagents were used in all steps prior to dialysis (once formed, fatty acid membranes act as a barrier to RNase).

Adding Micelles and Imaging. To prepare fatty acid micelle solutions, fatty acids were dissolved in 1 equiv of NaOH (final pH > 10), vortexed briefly, and agitated overnight under argon.[3] For the vesicle growth experiment in ammonium acetate, fatty acid micelle solutions were prepared by dissolving the fatty acid in 2 equiv of NH_4OH. Large (∼4 μm in diameter) multilamellar oleate vesicles (containing 2 mM HPTS) were prepared by large-pore dialysis, diluted 1:10 with the same buffer containing 0.8 mM oleic acid (to a final concentration of ∼1 mM oleic acid), and stored in an eppendorf tube. For the vesicle growth experiment, 5 equiv of oleate micelles were added to preformed vesicles, mixed, and then quickly pipetted into a disposable hemacytometer (Incyto, South Korea). These disposable hemacytometers are plastic microfluidic channels with small openings on the edge for sample loading. This design effectively prevents water evaporation and other perturbations during imaging. The addition of smaller quantities (1 equiv) of oleate micelles was performed using the same method. Vesicles with encapsulated fluorescent dyes were imaged using a Nikon TE2000S inverted epifluorescence microscope with extra long working distance (ELWD) objective lenses. The illumination source was a metal halide lamp (EXFO, Canada) with a 480 ± 20 nm (for HPTS) or a 546 ± 5 nm (for DY547) optical filter (Chroma, Rockingham, VT). The illumination intensity was kept low enough to avoid photobleaching using a set of two neutral density filters on the microscope. The images and movies were recorded using a digital camera (Hamamatsu Photonics, Japan) and postprocessed using Phylum Live software (Improvision, Lexington, MA). Confocal images were taken using a Leica SP5 AOBS scanning laser confocal microscope with Leica acquisition software (Leica, Germany). All images were cropped using Photoshop CS2 (Adobe Systems, San Jose, CA), with linear adjustments of brightness and contrast. All imaging studies were performed at room temperature, except for the studies on decanoate vesicles, which were performed at 50 °C.

Vesicle Growth and Division. Large (∼4 μm in diameter) multilamellar oleate vesicles (containing 2 mM HPTS) were prepared by the methods described above, diluted 1:300 with the same buffer (total oleic acid at ∼1 mM). Five equivalents of oleate micelles were added to the preformed vesicles, mixed, and then quickly pipetted into a depression on a cell-culture glass slide (Erie, Portsmouth, NH). The depression on the glass slide helps to hold the small volume of fluid and increase its stability during the imaging. The slide was covered by a homemade black-cardboard

(21) Berclaz, N.; Muller, M.; Walde, P.; Luisi, P. L. *J. Phys. Chem. B* **2001**, *105*, 1056–1064.
(22) Blochliger, E.; Blocher, M.; Walde, P.; Luisi, P. L. *J. Phys. Chem. B* **1998**, *102*, 10383–10390.
(23) Luisi, P. L.; Stano, P.; Rasi, S.; Mavelli, F. *Artif. Life.* **2004**, *10*, 297–308.
(24) Rasi, S.; Mavelli, F.; Luisi, P. L. *J. Phys. Chem. B* **2003**, *107*, 14068–14076.
(25) Rasi, S.; Mavelli, F.; Luisi, P. L. *Origins Life Evol. Biosphere* **2004**, *34*, 215–224.
(26) Luisi, P. L. *The emergence of life: from chemical origins to synthetic biology*; Cambridge University Press: Cambridge, 2006.
(27) Stano, P.; Wehrli, E.; Luisi, P. L. *J. Phys.: Condens. Matter* **2006**, *18*, S2231–S2238.
(28) Zhu, T.; Szostak, J. *PLoS ONE* **2009**, in press.

cover to avoid perturbations and evaporation during vesicle growth. After 20−25 min of imaging, we removed the cover and started to blow air briefly, at intervals, using a compressed air canister (Fisher, Hampton, NH) from 0.5 m away, until vesicle division occurred. Movies S1−S3 (Supporting Information) were recorded, processed, and exported using Phylum Live software. By cropping the images, we eliminated vesicle drifting within the ∼25 min period, for a better presentation of the main phenomenon. (No other nonlinear adjustments were made, and the uncropped, original movies are available upon request).

Vesicle Counting. An imaging assay was developed to count the total number of dye- or RNA-containing vesicles. A sample of 12 μL vesicle suspension was loaded into a disposable hemacytometer, which has a confined channel depth of 20 μm, and the total number of dye- or RNA-containing vesicles was counted from 20 nonoverlapping, randomly taken images. A Nikon TE2000S inverted epifluorescence microscope with 10 × CFI Plan Fluor ELWD DM objective lens was used for imaging. New vesicles that form de novo following micelle addition do not contain fluorescent dye or RNA, and since they cannot be observed by fluorescence microscopy, their formation does not affect the counting of the fluorescently labeled vesicles.

FRET Assay. The use of a FRET assay to measure surface area increase has been reported previously.[3,17,18] The assay measures the distance-dependent energy transfer between two fluorescent phospholipids anchored on the fatty acid vesicle membrane. As the membrane surface area increases by incorporating additional lipid molecules supplied as micelles, the FRET efficiency decreases, measured as an increase of donor fluorescence. FRET-dye-labeled vesicles were prepared by codissolving oleic acid, 0.2 mol % NBD-PE (*N*-(7-nitrobenz-2-oxa-1,3diazol-4-yl)-1,2-dihexadecanoyl-*sn*-glycero-3-phosphoethanolamine; excitation at 430 nm, emission at 530 nm), and 0.2 mol % Rh-DHPE (Lissamine Rhodamine B 1,2-dihexadecanoyl-*sn*-glycero-3-phosphoethanolamine; emission at 586 nm) in methanol before rotary evaporation and resuspension in buffer. The vesicle suspension was treated as described above for the preparation of large monodisperse vesicles. Large (∼4 μm in diameter) multilamellar FRET-dye-labeled vesicles were diluted 1:10 with the same buffer containing 0.8 mM oleic acid, to a final concentration of ∼1 mM oleic acid, and loaded into a measuring cuvette in a Cary Eclipse fluorimeter (Varian, Australia). Oleate micelles (5 equiv) were added to the cuvette 5 min after the recording had started. Immediately after addition of the micelles, a small volume of the vesicle suspension was removed from the cuvette, loaded into a disposable hemacytometer for microscopic observation, and incubated in parallel with the vesicles in the cuvette. After incubation for 30 min, the vesicle suspension in the cuvette was agitated using a pipet tip (instead of removing the cuvette for shaking) and allowed to stabilize for another 5 min before the second cycle of micelle addition. The addition of micelles and agitation causes artifactual intensity spikes, which were eliminated and replaced with break signs in Figure 2A. (The increasingly noisy relative surface area curve toward the end of the second cycle indicates that the measurement with the FRET assay is becoming less sensitive to the surface area changes at that range.) The control experiment of adding 5 equiv of NaOH (i.e., 5 mM final NaOH, which does not perturb the pH significantly due to the 0.2 M bicine buffer) was performed as described above. The increase of surface area of decanoate:decanol (2:1) vesicles during growth was measured using the same method. In this experiment, 2 equiv of decanoate micelles and 1 equiv of decanol emulsion were added to the decanoate:decanol (2:1) vesicles (in 0.2 M Na-bicine, pH 8.5, at room temperature, ∼20 mM initial amphiphile concentration). The decanol emulsion was made by dispersing decanol (with 1 mol % decanoate added) into 1 equiv of NaOH solution, followed by sonication. This method produced small droplets of relatively stable decanol emulsion (validated by microscopy; data not shown); without the addition of 1 mol % decanoate, the decanol droplets were much less stable, owing to interdroplet fusion.

Preparation of Unilamellar Fatty Acid Vesicles. The dehydration/rehydration method has been used for preparing unilamellar phospholipid vesicles,[29−31] and was adapted here for preparing unilamellar fatty acid vesicles. Oleate vesicles (in 0.2 M Na-bicine, pH 8.5, 5 mM oleic acid concentration with 0.2 mol % Rh-DHPE) were extruded through a polycarbonate membrane with 100-nm diameter pores. A sample of 5 μL of the vesicle suspension was placed on a glass slide (VWR, West Chester, PA), allowed to spread into a thin film (∼2-cm diameter area), and vacuum-dried overnight. After 10−15 min, 25 μL of buffer (0.2 M Na-bicine, pH 8.5; resulting in a final oleic acid concentration of ∼1 mM) was placed on the glass slide, and large unilamellar oleate vesicles formed.

Quantifying the Critical Shear Rate for Vesicle Division. Though wide-bore pipet tips were used to avoid excessive fluid shear, pipetting a vesicle suspension resulted in enough shear stress for some of the thread-like vesicles to divide, giving false positive results in vesicle counting. Therefore, we used the complete disappearance of the thread-like vesicles as an alternative indicator to confirm vesicle division. (In a control experiment where no fluid shear was applied, a large number of thread-like vesicles were present.) The disappearance of the thread-like vesicles is unlikely to be caused by lysis of vesicles as a result of shear stress, as the number of dye-labeled vesicles did indeed increase and no leakage of fluorescent dye was detected in these experiments. (Both the cone and plate of the viscometer are made of stainless steel and thus unlikely to disrupt the vesicle membrane through surface interactions.) A sample of 500 μL of large (∼4 μm in diameter) multilamellar oleate vesicles (containing 2 mM HPTS) was loaded into a cone−plate viscometer (Brookfield, Middleboro, MA), and 5 equiv of oleate micelles was added. After incubation for 30 min to allow for vesicle growth, the viscometer was started at a designated spinning speed (increased in successive trials) for 30 s. A sample was taken out from the vesicle suspension and loaded into a disposable hemacytometer to monitor vesicle division.

Cycles of Vesicle Growth and Division. In each cycle, 5 equiv of oleate micelles was added to large (∼4 μm in diameter) multilamellar oleate vesicles (containing 10 mM HPTS, in 0.2 M Na-glycine, pH 8.5, ∼1 mM initial oleic acid) in an eppendorf tube. After micelle addition, a small aliquot of vesicles was loaded into a disposable hemacytometer for microscopic observation and incubated in parallel with the vesicles in the eppendorf tube. After 30 min, the eppendorf tube was agitated briefly (by inverting the tube six times), and the vesicle shapes and sizes were monitored. A portion of the sample was then diluted 1:10 with buffer to a final concentration of ∼1 mM oleic acid to maintain this total oleic acid concentration at the beginning of each cycle. Before the start of the second cycle, 5 equiv of oleate micelles was added to the vesicles, allowing the vesicles to increase in volume and grow back to their original sizes in the absence of agitation for 24 h. The increase of vesicle volume dilutes the encapsulated fluorescent dye, and thus the contrast of the images in the second row of Figure 2B has been enhanced (the unenhanced original images are shown in Figure S3B). To quantify the number of dye-labeled vesicles and monitor the exponential increase of vesicle population, we repeated the growth and division of large (∼4 μm in diameter) multilamellar oleate vesicles (containing 10 mM HPTS, in 0.2 M Na-bicine, pH 8.5, ∼1 mM initial oleic acid) in three cycles but without allowing vesicle volume to increase (since the dilution of fluorescent dye would make such vesicles too dim for counting). Similarly to the procedures described above, the sample was diluted 1:10 with buffer

(29) Karlsson, M.; Nolkrantz, K.; Davidson, M. J.; Stromberg, A.; Ryttsen, F.; Akerman, B.; Orwar, O. *Anal. Chem.* **2000**, *72*, 5857–5862.
(30) Karlsson, A.; Karlsson, R.; Karlsson, M.; Cans, A. S.; Stromberg, A.; Ryttsen, F.; Orwar, O. *Nature (London)* **2001**, *409*, 150–152.
(31) Karlsson, M.; Sott, K.; Davidson, M.; Cans, A. S.; Linderholm, P.; Chiu, D.; Orwar, O. *Proc. Natl. Acad. Sci. U.S.A.* **2002**, *99*, 11573–11578.

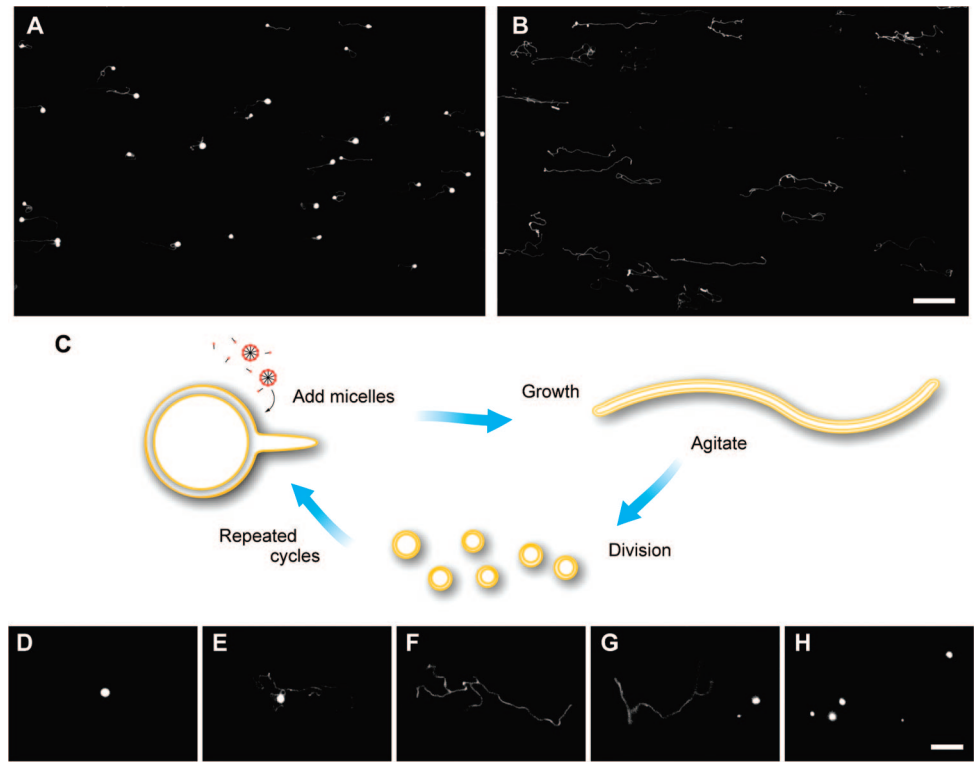

Figure 1. Vesicle growth and division. (A, B) Epifluorescence micrographs of vesicle shape transformations during growth, 10 and 30 min after the addition of 5 equiv of oleate micelles to multilamellar oleate vesicles (in 0.2 M Na-bicine, pH 8.5, ~1 mM initial oleic acid), respectively. All vesicles were labeled with 2 mM encapsulated HPTS, a water-soluble fluorescent dye, in their internal aqueous space. Scale bar, 50 μm. (C) Schematic diagram of cyclic multilamellar vesicle growth and division: vesicles remain multilamellar before and after division (shown as, but not limited to, two layers). (D−F) Growth of a single multilamellar oleate vesicle, 3 min, 10 min, and 25 min after the addition of 5 equiv of oleate micelles, respectively. (G, H) In response to mild fluid agitation, this thread-like vesicle divided into multiple smaller daughter vesicles (also shown in movie S1). Scale bar for D−H, 20 μm.

to a final concentration of ~1 mM oleic acid to maintain this total oleic acid concentration at the beginning of each cycle, and this dilution factor was later used to adjust the total vesicle count.

Measuring RNA Leakage. A small fraction of the vesicle suspension (less than 3% of the sample volume, to avoid vesicle disruption) was separated from intact vesicles by ultrafiltration in microcentrifuge tubes with 10 kDa cutoff filters. The fluorescence of 5′-DY547-labeled RNA (excitation at 557 nm, emission at 574 nm) was determined using a Cary Eclipse fluorimeter. RNA concentration levels of 0% and 100% were measured using vesicles before division, and vesicles after the addition of 1% Triton X-100, respectively.

Results

Vesicle Growth and Division. To observe the growth of multilamellar vesicles in real time, we prepared large monodisperse oleate (C18:1) vesicles (~1 mM initial oleic acid concentration) containing 2 mM encapsulated HPTS (8-hydroxypyrene-1,3,6-trisulfonic acid trisodium salt, a water-soluble, membrane-impermeable fluorescent dye). After the addition of 5 equiv (i.e., five times the initial amount of amphiphiles) of oleate micelles, a series of dramatic shape transformations occurred. The initially spherical vesicles first began to form thin tails that were only faintly fluorescent (Figure 1A). Over time, the spherical vesicles shrank and the tails grew in length and width as progressively more of the aqueous contents (labeled by fluorescent dye) migrated from the spherical vesicles into the tails. After ~30 min, the initially spherical vesicles had completely transformed into long thread-like vesicles with the dye-labeled aqueous contents more or less evenly distributed along the length of the filament (Figure 1B). No further shape transformation was observed for up to 2 h. Movies S1 and S2 show the transformation of vesicles from spherical to thread-like shape over a period of ~25 min after micelle addition. Whether vesicles were free-floating, or attached to a glass or plastic slide surface, we observed similar vesicle shape transformations. The shape transformations observed during growth were not altered by labeling the aqueous contents with a different fluorescent dye, calcein (bis[*N*,*N*-bis(carboxymethyl)-aminomethyl]fluorescein), or by labeling the membrane itself with a membrane-localized dye, Marina blue-DHPE (Marina Blue 1,2-dihexadecanoyl-*sn*-glycero-3-phosphoethanolamine) or Rh-DHPE (Lissamine Rhodamine B 1,2-dihexadecanoyl-*sn*-glycero-3-phosphoethanolamine). Finally, we observed the same growth-associated shape transformations with oleate vesicles ranging from 0.5 to 10 μm in diameter.

The highly elongated shape of the thread-like vesicles suggested that they might be sufficiently fragile to divide in response to mild shear forces, thus avoiding membrane rupture and subsequent contents release. To test this idea experimentally, we loaded a sample of large multilamellar oleate vesicles (containing 2 mM HPTS, ~1 mM initial oleic acid) into a single-depression glass slide, added 5 equiv of oleate micelles, and allowed ~25 min for the vesicles to grow into thread-like shapes (Figure 1D−F; Figure S1A,B, Supporting Information; movies S1 and S2). We then gently agitated the vesicle suspension by repeatedly blowing puffs of air onto the sample from a distance of about 0.5 m using a compressed air canister. We observed that the thread-like vesicles divided into multiple smaller spherical daughter vesicles (Figure 1G,H; Figure S1C,D; movies S1 and S2). These daughter vesicles were distinctly separate

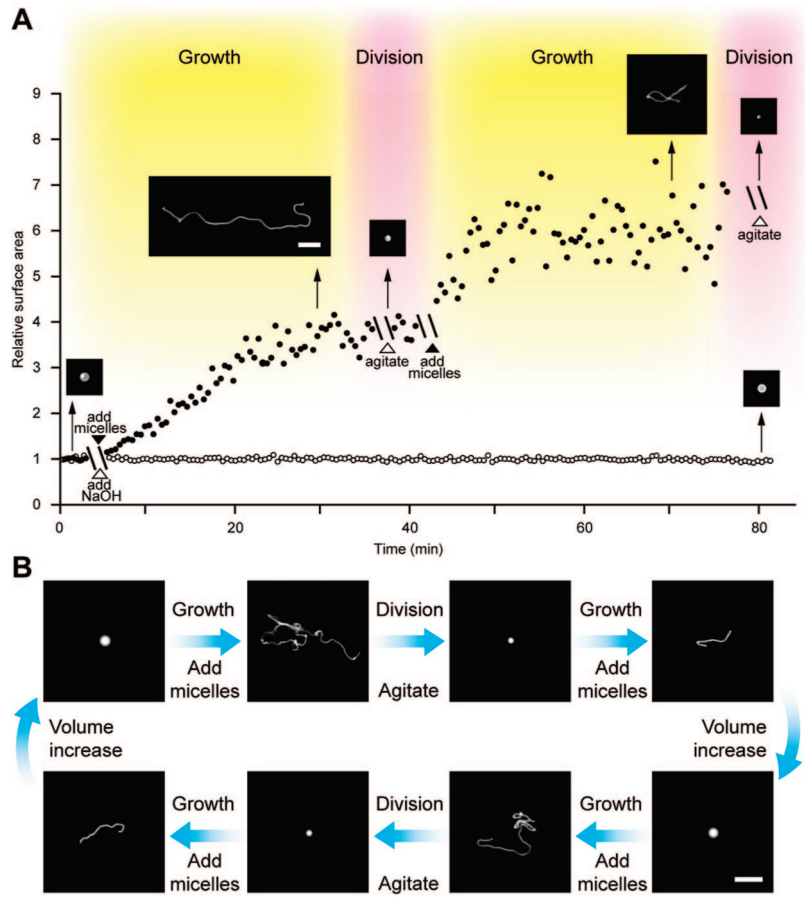

Figure 2. Cycles of vesicle growth and division. (A) Relative surface area after two cycles of addition of 5 equiv of oleate micelles (solid circles) or 5 equiv of NaOH (open circles) to oleate vesicles, each followed by agitation. Inset micrographs show vesicle shapes at indicated times. Scale bar, 10 μm. (B) Vesicle shapes during cycles of growth and division in a model prebiotic buffer (0.2 M Na-glycine, pH 8.5, ~1 mM initial oleic acid, vesicles contain 10 mM HPTS for fluorescence imaging). Scale bar, 20 μm.

from each other, gradually moving apart in random directions by Brownian motion. The daughter vesicles were brightly fluorescent, showing that most of the encapsulated contents were retained during division. To quantify the fluid shear required for the division of thread-like vesicles, we used a cone−plate viscometer to measure the critical shear rate under controlled fluid shear. The critical shear rate for thread-like vesicle division was 15 s^{-1}, corresponding to a shear stress of 0.35 dynes/cm^2 (fluid viscosity measured 2.3 cP). Higher shear rates, up to 1500 s^{-1}, also led to division without disrupting the vesicles.

Having observed efficient growth and division following the addition of 5 equiv of fatty acid to preformed vesicles, we asked whether efficient division could still occur following a smaller extent of growth. When vesicles were fed with smaller quantities of micelles (1 equiv), they grew to the sphere-tail intermediate stage, at which point gentle agitation was still able to induce division (Figure S2). In contrast, without micelle addition, vesicles remained spherical and were unable to divide by gentle agitation alone (Figure S2I). Vesicle division at the sphere-tail intermediate stage did not occur by simple "tearing-off" of the tail but rather through redistribution of the encapsulated contents into the widening tail portion, followed by division into multiple progeny vesicles (Figure S2B−E; movie S3). As observed by confocal microscopy, the majority of daughter vesicles were multilamellar after division. Hence, when only small quantities of micelles are added, and fluid agitation is present at the sphere-tail intermediate state of growth, vesicles can still divide into multiple progeny.

We determined the efficiency of fatty acid incorporation into growing vesicles by measuring the increase in vesicle surface area by two independent methods. First, we measured the surface area of individual vesicles before and after growth by analyzing high-resolution images; the results are approximate but suggest an increase of surface area by ~4-fold following the addition of 5 equiv of oleate micelles to oleate vesicles (text S1). We then used a fluorescence assay based on Förster resonance energy transfer (FRET) to monitor the growth of oleate vesicles labeled by donor and acceptor membrane dyes.[3,18,19] After the addition of 5 equiv of oleate micelles, we took a small sample out of the measuring cuvette and observed the vesicles growing into thread-like shapes on a glass slide (Figure 2A, micrographs). Meanwhile, we observed increasing donor fluorescence, corresponding to increasing membrane surface area, in the remainder of the sample. The membrane surface area increased by ~3.7-fold at 25 min after the addition of 5 equiv of oleate micelles (Figure 2A). Thus both microscopic and FRET data suggest a 50−60% efficiency of incorporation of added fatty acid into preformed vesicles by this growth pathway, which is consistent with the results from previous studies.[18]

Cycles of Growth and Division. Having demonstrated both growth and division of large multilamellar vesicles, we proceeded to examine multiple cycles of vesicle growth and division. First, we monitored two rounds of oleate vesicle growth and division using the FRET assay to confirm the increase in membrane surface area in both growth phases and microscopy to monitor the shape transformations and division in both cycles

(Figure 2A, micrographs). We then tested complete cycles of vesicle growth and division in a more prebiotically plausible buffer: glycine, the most abundant of the many amino acids found in a wide range of Miller−Urey-type prebiotic synthesis experiments.[32,33] We monitored two cycles of vesicle growth and division and observed that in each cycle, oleate vesicles (containing 10 mM HPTS, in 0.2 M Na-glycine, pH 8.5, ~1 mM initial oleic acid) grew into thread-like shapes after the addition of 5 equiv of oleate micelles and divided into spherical progeny after agitation (Figure 2B). Between each cycle, after the addition of 5 equiv of micelles and in the absence of agitation for 24 h, the slowly permeable solute, glycine, equilibrates across the vesicle membranes, allowing the vesicles to increase in volume (Figure 2B; Figure S3). In a true protocell containing a replicating genome, the replication of the genome could also contribute to the osmotically driven volume recovery between cycles of growth and division.[17] Finally, we used an imaging assay to count the number of daughter vesicles containing fluorescent dye, in order to monitor the vesicle population over three cycles of growth and division in bicine (*N,N*-bis(2-hydroxyethyl)glycine) buffer (without volume recovery, which would dilute the fluorescent dye and compromise the counting assay). We found that the vesicle count increased exponentially ($r^2 > 0.99$) (Figure S4), as would be expected if the efficiency of growth and division was constant in each cycle.

We were interested in whether the protocell growth and division cycle described above might also function in a more prebiotically plausible chemical environment and, thus, might represent a possible pathway for the reproduction of early protocells. We therefore prepared oleate vesicles (containing 2 mM HPTS, ~1 mM initial oleic acid) in a mixture of amino acids (60 mM glycine, 30 mM alanine, 10 mM aspartate, and 10 mM glutamate, pH 8.5) that partially mimics the outcome of Miller−Urey-type experiments,[32,33] as well as amino acids found in carbonaceous chondrite meteorites.[34] (Volatile compounds such as ammonia and acetic acid cannot accumulate to high concentrations.) We observed similar growth and division of vesicles in this mixed amino acid solution (Figure 4A,E). We also observed similar growth and division of oleate vesicles in glycinamide buffer and in Tris buffer (both at pH 8.5; data not shown), which, together with the previously described results, indicates that vesicle growth and division can occur under a variety of solution conditions.

Growth and Division of RNA-containing Model Protocells. To mimic protocells containing a nucleic acid genome and test the redistribution of encapsulated genetic molecules into daughter vesicles after division, we prepared oleate vesicles containing encapsulated RNA molecules (DY547-A_{10}, dye-labeled polyadenylic acid, 0.5 mM). We then repeated the vesicle growth experiment by adding 5 equiv of oleate micelles to the preformed oleate vesicles and observed the same vesicle shape transformations as previously seen with dye-labeled vesicles (Figure 3A,B). We next monitored vesicle division with redistribution of encapsulated RNA molecules into progeny using the vesicle counting assay. After induction of division by agitation, we observed a ~6-fold increase in vesicle count (Figure 3C), just as seen previously with dye-labeled vesicles. After division, only a trace amount of RNA leakage from vesicles was detected (Figure 3D). In contrast, the artificial means of vesicle division by extrusion is much less efficient in that ~40% of the encapsulated RNA leaked out.

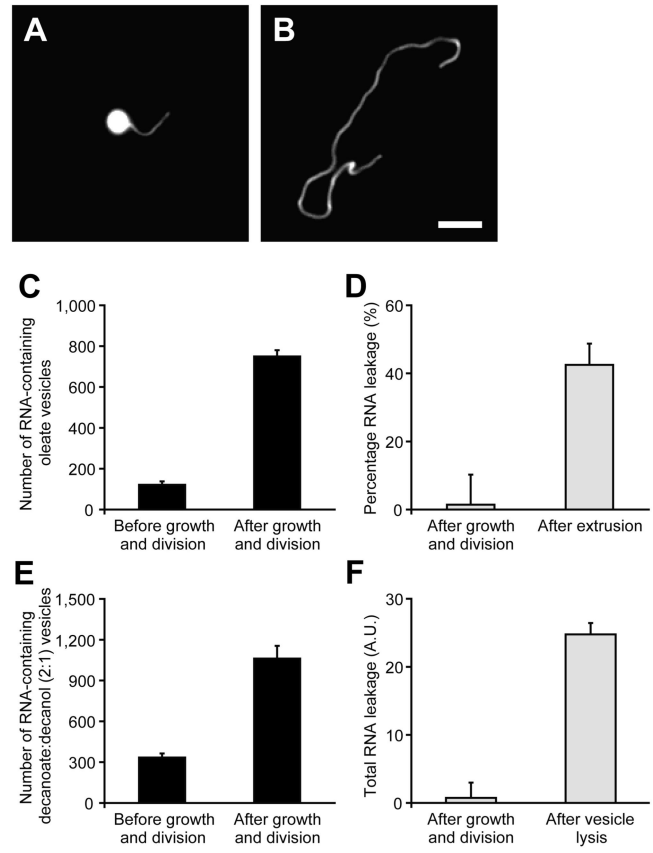

Figure 3. Growth of vesicles containing encapsulated RNA, and redistribution of RNA molecules into daughter vesicles. (A, B) Oleate vesicle (in 0.2 M Na-bicine, pH 8.5, ~1 mM initial oleic acid) containing 5′-DY547-labeled RNA (DY547-A_{10}, 0.5 mM) at 10 and 30 min after the addition of 5 equiv of oleate micelles, respectively. Scale bar, 10 μm. (C) Number of RNA-containing oleate vesicles before and after division, $n = 3$. (D) Percentage RNA leakage after the division of thread-like oleate vesicles by agitation, versus the leakage from 4-μm diameter vesicles extruded through 2 μm pores, $n = 3$. (E) Number of RNA-containing decanoate:decanol (2:1) vesicles (in 0.2 M Na-bicine, pH 8.5, at room temperature, ~20 mM initial amphiphile concentration) before and after division, $n = 3$. (F) Total amount of RNA leakage from decanoate:decanol (2:1) vesicles after division, versus the leakage from vesicles lysed by adding 1% Triton X-100, $n = 3$.

Prebiotically Plausible Protocell Membranes. Although oleate vesicles are an excellent model system for the study of protocell membranes,[3,9,17,19] shorter-chain, saturated fatty acids are more likely components of prebiotic membranes. We therefore examined the growth and division of multilamellar vesicles composed of two shorter-chain fatty acids: myristoleic (C14:1) and decanoic (C10:0) acids. After the addition of 5 equiv of the corresponding fatty acid micelles, these vesicles grew into thread-like shapes (Figure 4B,C). They also divided, as expected, upon gentle agitation (Figure 4F,G).

Prebiotic vesicles were most likely composed of mixtures of amphiphiles. Notably, many such mixtures, such as decanoate:decanol (2:1), generate vesicles that are stable under a wider range of pH and ionic conditions, and are more permeable to nutrient molecules than pure fatty acid vesicles.[5,17] However, a 2:1 decanoate:decanol mixture does not form micelles at high pH, and it was therefore necessary to investigate alternative means of feeding such vesicles. We found that a combination

(32) Miller, S. L. *Science* **1953**, *117*, 528–9.
(33) Miller, S. L.; Urey, H. C. *Science* **1959**, *130*, 245–51.
(34) Kvenvolden, K.; Lawless, J.; Pering, K.; Peterson, E.; Flores, J.; Ponnamperuma, C.; Kaplan, I. R.; Moore, C. *Nature (London)* **1970**, *228*, 923–6.

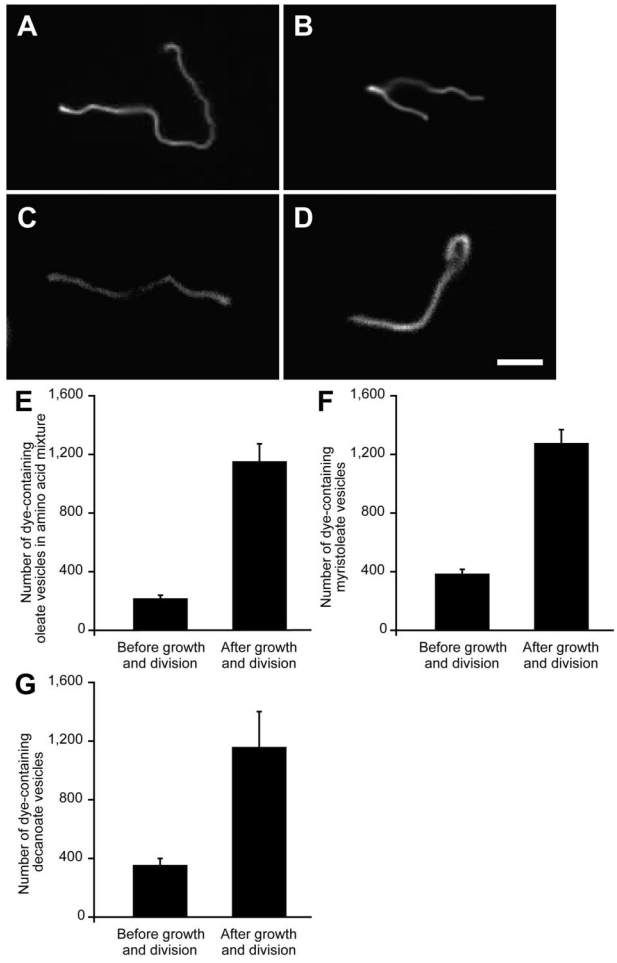

Figure 4. Vesicle growth and division in various buffers and with various lipid compositions (A) Oleate vesicle (containing 2 mM HPTS, in 60 mM Na-glycine, 30 mM Na-alanine, 10 mM Na-aspartate, and 10 mM Na-glutamate, pH 8.5, ~1 mM initial oleic acid) at 30 min after the addition of 5 equiv of oleate micelles. (B) Myristoleate vesicle (containing 2 mM HPTS, in 0.2 M Na-bicine, pH 8.5, ~4 mM initial myristoleic acid) at 30 min after the addition of 5 equiv of myristoleate micelles. (C) Decanoate vesicle (containing 2 mM HPTS, in 0.2 M Na-bicine, pH 7.4, at 50 °C, ~60 mM initial decanoic acid) at 30 min after the addition of 1.7 equiv of decanoate micelles. (D) Decanoate:decanol (2:1) vesicle (containing 2 mM HPTS, in 0.2 M Na-bicine, pH 8.5, at room temperature, ~20 mM initial amphiphile concentration) at 30 min after the addition of 2 equiv of decanoate micelles and 1 equiv of decanol emulsion. Scale bar for A−D, 10 μm. (E) Number of dye-containing oleate vesicles in a mixed amino acid solution (conditions as above) before and after growth and division, $n = 3$. (F) Number of dye-containing myristoleate vesicles (conditions as above) before and after growth and division, $n = 3$. (G) Number of dye-containing decanoate vesicles (conditions as above) before and after growth and division, $n = 3$.

of decanoate micelles and decanol emulsion led to efficient growth of 2:1 decanoate:decanol vesicles (Figure 4D and Figure S5), which were able to divide and redistribute the encapsulated RNA molecules into daughter vesicles without significant leakage (Figure 3E,F). Finally, when we added oleate micelles to POPC (1-palmitoyl-2-oleoyl-*sn*-glycero-3-phosphocholine) vesicles, which are more closely related to modern cell membranes and can maintain a pH gradient across the membrane,[19] they also went through similar shape transformations. These observations suggest that the growth of multilamellar vesicles through a series of shape transformations is a phenomenon that occurs with vesicles composed of a wide variety of lipids and lipid mixtures.

Mechanism of Initiation of Filamentous Vesicle Growth. The increased vesicle surface area that follows the addition of micelles must, in the absence of a corresponding volume increase, lead to a change in vesicle shape. As shown above, when micelles are added quickly to preformed vesicles, vesicle surface area increases rapidly (Figure 2A). Since the buffer solutes (e.g., bicine, glycine, or other amino acids) are impermeable to oleate membranes on this time scale,[19] the vesicle volume cannot increase through the equilibration of external and internal solutes. Estimates of vesicle volume derived from the analysis of high-resolution optical images are consistent with this prediction (text S1). In comparison, previous studies of reduced volume (e.g., subspherical) phospholipid vesicles have shown that a wide variety of shapes can be generated, such as vesicles with bead-like protrusions,[35] as summarized in shape versus volume phase diagrams.[36,37] However, none of these forms resembles the growth intermediate of a spherical vesicle decorated with one or two thin tail-like protrusions that we have observed.

To account for the unusual growth mode that we observed, we hypothesized that during the early stages of vesicle growth, the added fatty acid molecules first encounter the outermost membrane, which therefore grows faster than the inner membrane layers. Since the volume between the outermost membrane and the inner membrane layers (intermembrane volume) is small and cannot increase on the time-scale of membrane surface growth, the outermost membrane can only grow by forming protrusions (Figure 5A). At later times, the inner membrane layers may also grow and spread throughout the growing thread-like vesicle. To test this idea, we first asked whether the multilamellar structure of vesicles was essential for the formation of thin tail-like protrusions during growth. We began by examining our initial spherical vesicles and sphere-tail growth intermediates by confocal microscopy, using a membrane-localized fluorescent dye to image the vesicle membranes. The initially spherical vesicles were clearly multilamellar (Figure 5B). At ~10 min after micelle addition, one or a few of the outer membrane layers formed a tail-like protrusion, while the inner membrane layers remained spherical (Figure 5C). After division, the daughter vesicles remained multilamellar, allowing for subsequent cycles of efficient growth and division to occur with the multilamellar progeny (Figure 5D). To directly test the hypothesis that the multilamellar structure of vesicles played an important role in their shape transformations following micelle addition, we prepared unilamellar oleate vesicles by a modified dehydration/rehydration method.[29,30] We observed that, in contrast to the growth of multilamellar vesicles, unilamellar vesicles elongated symmetrically into tubular shapes without forming tails during growth (Figure 5G).

Finally, we further tested the hypothesis that the vesicle shape transformation through sphere-tail growth intermediates is a consequence of volume conservation, due to the slow permeability of buffer solutes. We prepared large multilamellar oleate vesicles in ammonium acetate (0.2 M, pH 8.5) buffer, a solute that is highly permeable to vesicle membranes as a result of its equilibrium with ammonia (NH_3) and acetic acid (CH_3COOH) (Figure 6A). The rapid permeation of these neutral species

(35) Bozic, B.; Gomiscek, G.; Kralj-Iglic, V.; Svetina, S.; Zeks, B. *Eur. Biophys. J.* **2002**, *31*, 487–96.
(36) Dobereiner, H. G. In *Giant Vesicles*; John Wiley and Sons, Inc.: New York, 2000.
(37) Dobereiner, H. G. *Curr. Opin. Colloid Interface Sci.* **2000**, *5*, 256–263.

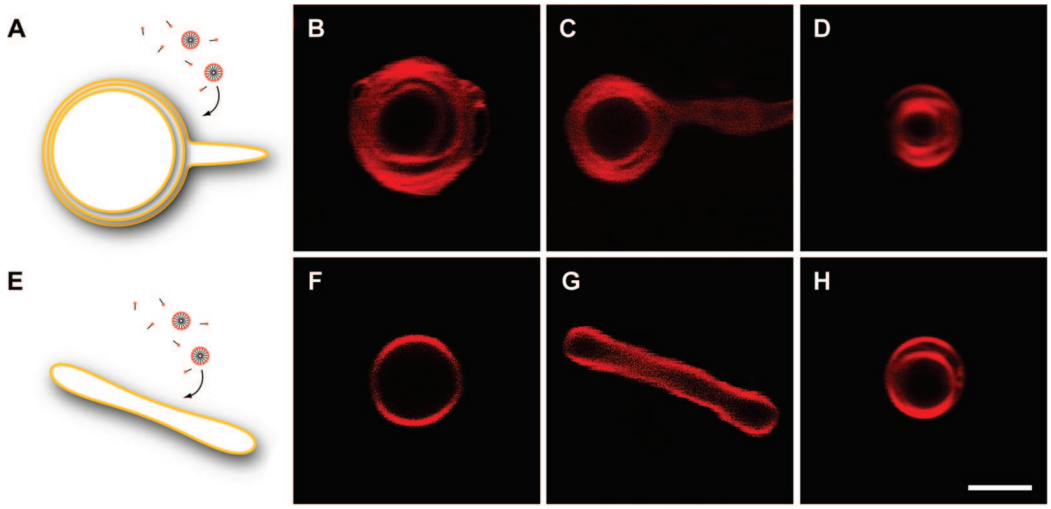

Figure 5. Growth of multilamellar versus unilamellar vesicles (A) Schematic diagram of incorporation of micelles into a multilamellar vesicle: the outermost membrane grows faster than the inner membrane layers. (B, C) Confocal images of multilamellar oleate vesicle (0.2 mol % Rh-DHPE, in 0.2 M Na-bicine, pH 8.5, ~1 mM initial oleic acid) before and 10 min after the addition of 1 equiv of oleate micelles, respectively. (D) Confocal image of multilamellar vesicle after division. (E) Schematic diagram of incorporation of micelles into a unilamellar vesicle. (F, G) Confocal images of unilamellar oleate vesicle (conditions as above) before and 10 min after the addition of 1 equiv of oleate micelles, respectively. (H) Confocal image of a multilamellar vesicle formed after the agitation of elongated unilamellar vesicles. Scale bar for B−D, F−H; 2 μm.

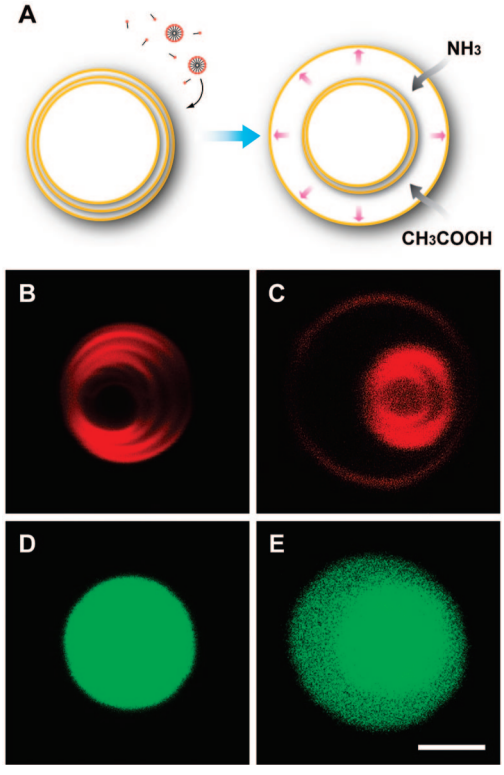

Figure 6. Vesicle growth in a highly permeable buffer (A) Schematic diagram of growth of a multilamellar vesicle in ammonium acetate: as the surface area of the outermost membrane increases, the solutes in their neutral forms (NH_3 and CH_3COOH) permeate the membrane, allowing the internal volume to increase. (B, C) Confocal images of multilamellar oleate vesicle (0.2 mol % Rh-DHPE, in 0.2 M ammonium acetate, pH 8.5, ~1 mM initial oleic acid) before and 10 min after the addition of 1 equiv of oleate micelles, respectively. (D, E) Confocal images of multilamellar oleate vesicle (containing 2 mM HPTS, in 0.2 M ammonium acetate, pH 8.5, ~1 mM initial oleic acid) before and 10 min after the addition of 1 equiv of oleate micelles, respectively. Scale bar for B−E, 2 μm.

allows vesicle volume to increase significantly during growth, resulting in maintenance of spherical vesicle shapes and the complete absence of formation of sphere-tail intermediates. By confocal microscopy, we observed that the growth of the outermost membrane had indeed outpaced that of the inner membrane layers, such that the intermembrane volume increased significantly (Figure 6C). When multilamellar oleate vesicles containing 2 mM HPTS (a membrane-impermeable dye) grew in ammonium acetate buffer, the fluorescence intensity in the intermembrane space decreased due to the dilution of the fluorescent dye, reflecting the influx of solutes and water into the intermembrane space (Figure 6E).

Discussion

The pathway for protocell growth and division that we have described is robust, in that it operates over a wide range of lipid compositions, solutes, shear rates, and vesicle sizes. This allows for considerable flexibility in the design of more complete or sophisticated protocell models involving the integration of replicating membrane and genetic systems. In this new pathway, growth and division are naturally coupled, in that growth leads to the formation of fragile thread-like vesicles that are predisposed to divide. In a fluid environment of modest shear forces, growth inevitably leads to division, so that no additional built-in mechanism is needed to coordinate growth and division. Such coupling of growth and division constitutes a significant simplification for efforts to map out a pathway for the synthesis of artificial forms of cellular life. On the other hand, many of the physical properties of model protocell membranes such as permeability,[5,20] thermostability,[6] and competition[17] have so far been examined only with small unilamellar vesicles, and thus we are currently re-examining these properties in the context of large multilamellar vesicles.

A population of growing and dividing vesicles, while reminiscent of a population of growing and dividing cells, cannot evolve to the greater complexity required for adaptation to a changing environment without some form of heritable genetic information. A complete model of a simple protocell therefore requires the addition of a genome that can replicate within the membrane-bound compartment and be inherited by daughter protocells. The pathway for protocell growth and division shown here allows short RNA strands dissolved in the aqueous contents

of parental vesicles to be randomly redistributed into their daughter vesicles in amounts proportional to their volume, without significant leakage. This pathway is compatible with several distinct models of protocell genome replication, such as ribozyme-catalyzed RNA replication,[2] or spontaneous chemical replication,[5] where short strands of RNA, DNA, or perhaps some other genetic polymer constitute the genome. Any catalytically or structurally useful genetic polymer that promoted faster protocell self-replication would tend to increase in frequency within a population of growing and dividing vesicles, providing a possible route for the emergence of Darwinian evolutionary behavior among protocells.[1,17]

We suggest that the simplicity of the conditions required for artificial protocell growth and division makes it plausible that similar processes might have occurred on the early Earth. Repeated cycles of growth and division, in which both the parental membrane material and aqueous contents are transmitted to progeny, could have been a common phenomenon in environments providing an episodic source of fatty acids to an aqueous reservoir. The energy source for the division of thread-like vesicles is simply the kinetic energy of mildly agitated liquid water which is common in many natural environments. These conditions are far simpler than might have been expected in view of the remarkable complexity of modern cellular growth and division and are simpler than those proposed in previous models.[1,3,4] While specific scenarios are easy to imagine (vesicles in a wind-agitated pond, fed with fatty acid micelles from an alkaline hot spring source of fatty acids synthesized by Fischer−Tropsch type chemistry at depth), they are poorly constrained because of our lack of detailed knowledge of plausible pathways for prebiotic fatty acid synthesis, which should be a priority for future studies in prebiotic chemistry.

Our experiments lead to a series of intriguing questions concerning protocell membranes, e.g., why only one or two tail-like protrusions emerge from a growing vesicle, and what forces drive the transfer of fatty acids from the outermost to inner membrane layers at the later stage of vesicle growth, resulting in their elongation into thread-like shapes. With respect to division, it is important to determine the mechanism of the shear-induced division of thread-like vesicles, e.g., whether the tension-induced pearling instability[38] plays a role (text S1; Figure S1C; movie S2). A better understanding of the underlying mechanisms will facilitate the design of artificial living systems and may also lead to greater insight into the origin of cellular life.

Acknowledgment. We thank R. Bruckner, I. Chen, S. Chung, M. Elenko, R. Irwin, P. L. Luisi, A. Luptak, S. Mansy, D. Treco, C. Wong, and S. Zhou for helpful discussions and comments on the manuscript. This work was supported in part by grant EXB02-0031-0018 from the NASA Exobiology Program. J.W.S. is an Investigator of the Howard Hughes Medical Institute.

Supporting Information Available: Text S1 with references, Figures S1−S6, and movies S1−S3. This material is available free of charge via the Internet at http://pubs.acs.org.

JA900919C

(38) Bar-Ziv, R.; Moses, E. *Phys. Rev. Lett.* **1994**, *73*, 1392–1395.